Vol. 92 No. 6 pp. 2067–2078 ACTA GEOLOGICA SINICA (English Edition) Dec. 2018

Magnetochronology of Late Miocene Mammal Fauna in Xining Basin, NE Tibetan Plateau, China

HAN Jian'en[1], SHAO Zhaogang[1, *], CHEN Qiguang[1], XU Biao[1, 2], ZHANG Qianqian[1], YU Jia[1], MENG Qingwei[3], ZHANG Xuefeng[4], WANG Jin[1] and ZHU Dagang[1]

1 *Institute of Geomechanics, Chinese Academy of Geological Sciences, Beijing 100081, China*
2 *China University of Geosciences (Beijing), Beijing 100083, China*
3 *Chinese Academy of Geological Sciences, Beijing 100037, China*
4 *Yellow River Conservancy Technical Institute, Kaifeng 475004, Henan, China*

Abstract: The Xining basin is located in the northeastern margin of the Qinghai-Tibet Plateau. It is a rift basin formed in Mesozoic and Cenozoic and structurally belongs to the intersection of Kunlun and Qilian Mountains. Cenozoic fluvial and lacustrine sedimentary strata are continuous in the Xining basin, with a thickness of more than 800 m, completely recording the deformation uplifting, weathering and denudation history and climate change process of the northeastern plateau. Currently, early Miocene Xijia fauna, early Middle Miocene Danshuilu fauna and late Middle Miocene Diaogou fauna are discovered in the Xining basin, which provide an important basis for the stratigraphic correlation of the Cenozoic strata in the Xining basin. However, in the next few decades, there are no reports about the large mammal fossils in the Xining basin, especially about late Miocene fauna. The author discovered a large amount of mammal fossils in the Neogene sedimentary strata in Huzhu area, Xining basin. According to the identification results of the Institute of Vertebrate Paleontology and Paleoanthropology, Chinese Academy of Sciences, these fossils mainly included *Hipparion dongxiangense, Chilotherium* sp., *Parelasmotherium* sp., *Stephanocemas* sp. *and Kubanochoerus* sp. and their age was early Late Miocene. Since the discovery of this set of fossils directly filled the blank that there were no large mammal fossils in the Xining basin in Late Miocene, it was very important for studying the magnetic stratigraphic chronology of fossil-forming strata and establishing the paleomagnetic chronology scale plate of mammal fossils. In this paper, the paleomagnetic data of the fossil-forming stratigraphic profile, Banyan profile, were measured and the paleomagnetic records were collected through high density sampling, and finally the paleomagnetic polarity column of the profile was established. The results showed that five positive and five negative polarity segments were recorded in Banyan profile, which corresponded well to the polarity between C3Br.1n-C4n.2n in the standard polarity column. The age of profile top was about 7.25 Ma and profile bottom was about 8.4 Ma, with an age range of 1.15 Ma. The mammal fossils discovered this time were exposed between positive and negative polarities N5 and R5 at the bottom of the profile, corresponding to C4r.1r at negative polarity and C4n.2n at positive polarity in the standard polarity column. The age of mammal fossils was about 8.3 Ma. The paleomagnetic chronology of the strata and paleontological fossils determined the absolute age of late Miocene mammal fossils and expanded the upper age of late Miocene Xianshuihe Formation (N_1xn) in the Xining basin, which had provided new basic data for further studying the stratigraphic deposition and correlation of late Cenozoic strata and regional environmental evolution.

Key words: mammal fossils, magnetic stratigraphy, late Miocene, Xining basin, Qinghai-Tibet Plateau

1 Introduction

The Xining basin is located in the northeastern margin of the Qinghai-Tibet Plateau. It is a rift basin formed in Mesozoic and Cenozoic and structurally belongs to the intersection of Kunlun and Qilian Mountains. Cenozoic fluvial-lacustrine sedimentary strata are continuous in the Xining basin, with a thickness of more than 800 m,

* Corresponding author. E-mail: hanjianen@163.com

completely recording the deformation uplifting, weathering and denudation history and climate change process of the northeastern plateau. In recent decades, the magnetic stratigraphy of sedimentary strata (Horton et al., 2004; Wu Lichao et al., 2006; Dai et al., 2006; Fang Xiaomin et al., 2007; Dupont-Nivet et al., 2007; Xiao et al., 2010, 2012; Abels et al., 2011; Bosboom et al., 2014; Zan et al., 2015), the wood fossils (Chen Chuanfei et al., 2009), the paleoclimate of Eocene-Miocene (Sun Xiuyu et al., 1984; Xu Li et al., 2009) in the Xining basin have been studied. Currently, early Miocene Xijia fauna, early Middle Miocene Danshuilu fauna and late Middle Miocene Diaogou fauna are discovered in the Xining basin (Liu Mengru, 1992), which provides an important basis for the stratigraphic correlation of the Cenozoic strata in the Xining basin. However, in the next few decades, there are no reports about the large mammal fossils in the Xining basin, especially about late Miocene fauna.

Since 2015, the author discovered a large amount of mammal fossils in the Neogene sedimentary strata in Jiangjiagou in Huzhu area and Shagou in Banyan Village, Xining basin (Han Jian'en et al., 2015, 2017). According to the identification results of the Institute of Vertebrate Paleontology and Paleoanthropology, Chinese Academy of Sciences, these fossils were *Hipparion dongxiangense, Chilotherium* sp., *Parelasmotherium* sp., *Stephanocemas* sp. and *Kubanochoerus* sp. and their age was early Late Miocene. Since the discovery of these fossils directly filled the blank that there were no large mammal fossils in the Xining basin in late Miocene, it was very important for studying fossil-forming strata and establishing the paleomagnetic chronology scale plate of mammal fossils. Therefore, aimed at the fossil-discovering strata in northern Xining basin, the paleomagnetic chronology of late Miocene fluvial-lacustrine strata was studied, the paleomagnetic chronology scale plate of the strata and paleontological fossils was established, the absolute age of late Miocene mammal fossils was determined and the upper age of Xianshuihe Formationin in the Xining basin was expanded, which had provided new basic data for further studying the stratigraphic deposition, paleontology evolution of the Xining basin in late Miocene and uplifting environmental comparison.

2 Regional Geological Background

The Xining basin is located in the northeastern margin of the Qinghai-Tibet Plateau. It is a rift basin formed in Mesozoic and Cenozoic and structurally belongs to the intersection of Kunlun and Qilian Mountains, with Laji Mountain fault zone to the south, Daban Mountain fault zone to the north, Riyue Mountain fault zone to the west and the Longdong basin in Gansu Province to the east (Fig. 1).The bedrocks of the basin and its surrounding mountains are Sinian, Cambrian, Ordovician, Silurian, Triassic and Caledonian granitoid (Bureau of Geology and Mineral Resources of Qinghai Province, 1991).

As a typical representative of Cenozoic sedimentary basins in the northeastern margin of the Qinghai-Tibet Plateau, the Xining basin has continuously attracted the concern of the experts and scholars of geology and paleontology. In 1885, Loczy named a set of red foothills fluvial-lacustrine deposits as "Guide Series" or "Guide Buildup" and determined their age as Pliocene based on the discovery of *Myospalax arvicolinus*. In 1965, Qinghai Regional Survey team named the Miocene sediments and Pliocene sediments as "Xining Formation" and "Guide Formation", respectively. Based on regional geological survey and micro-paleontological fossil data, Qinghai Petroleum Reconnaissance Team named the Miocene sediments and Pliocene sediments as "Xining Group" and "Guide Group" to represent Paleogene and Neogene (Ye Liusheng, 1976a, 1976b; Bureau of Geology and Mineral Resources of Qinghai Province, 1991). Based on sporopollen fossils and vertebrate fossils, Huang Youyuan (1977) divided Lower Tertiary into Qijiachuan Formation, Honggou Formation and Mahalagou Formation from bottom to top and Upper Tertiary into Xiejia Formation and Chetougou Formation (Huang Youyuan, 1977). "Strata Generality of China" divided Upper Tertiary into Xiejia Formation, Chetougou Formation, Xianshuihe Formation and Linxia Formation from bottom to top (Chinese Academy of Geological Sciences, 1982). Based on fine paleomagnetic chronology, paleontological fossil and tectonic and sedimentary cycle, Fang Xiaomin et al. (2007) divided Xining Group into Qijiachuan Formation (E_1q), Honggou Formation (E_2h), Mahalagou Formation (E_3m), Xiejia Formation of Guide Group (N_1x), Chetougou Formation (N_1c), Xianshuihe Formation (N_1xn) and Linxia Formation (N_2l) from bottom to top. In general, the lower strata are composed of Paleogene purplish red-orange glutenite, sandstone, siltstone and mudstone. The mudstone in the middle part is interbeded with a large set of gypsum. The middle strata are composed of variegated (brownish red, grayish green and brownish yellow) mudstone and siltstone, interbeded with sandstone and bluish gray marl. The upper strata are composed of grayish black conglomerate, boulder conglomerate, with Quaternary grayish green, grayish yellow siltstone at top (Fang Xiaomin et al., 2007). Due to the erosion at the top of stratigraphic profile, the paleomagnetic age of Xianshuihe Formation is only about 17 Ma. The distribution of each formation in the basin is shown in Fig. 1.

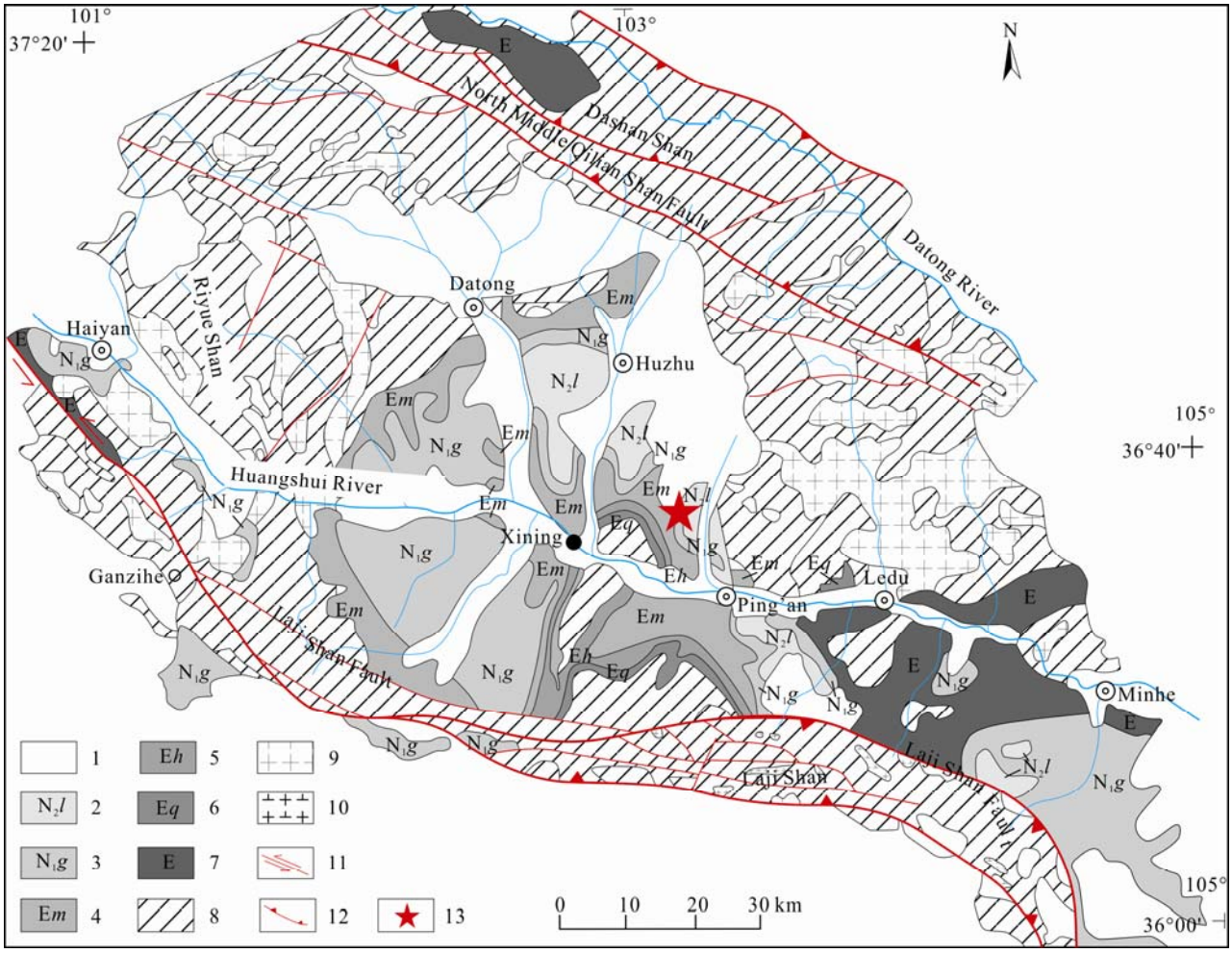

Fig. 1. Geological map and the location of the fossil (modified from Dai et al., 2006).
1, Quaterary; 2, Linxia Group; 3, Guide Group; 4, Mahalagou Formation; 5, Honggou Formation; 6, Qijiachuan Formation; 7, Eocene; 8, Precambrian-Mesozoic; 9, granite; 10, granodiorite; 11, strike-slip fault; 12, thrust fault; 13, section position.

3 Method and Results

3.1 Stratigraphic profile

Fossils were discovered in the same formation in Jiangjiagou in Huzhu County and Shagou in Banyan Village. Detailed stratigraphic profile survey was carried out aimed at well exposed Shagou profile in Banyan Village. The geographical coordinates were N36°41'17.0", E102° 6'2.0", the elevation was 2645 m (hereinafter referred to as Banyan profile) and the thickness was 46m (Fig. 2). The stratigraphic profile was measured and its lithology was as follows :

Overlying strata: conglomerate

·····Conformity·····

1. 0–10.6 m Brownish yellow, yellowish brown thick mudstone, tight and massive, bedding is not developed, interbeded with glutenite thin layer 10.6 m

2. 10.6–12.6 m gray conglomerate, gravel is dominated by quartzite and siliceous rock, with minor limestone, gravel diameter ranges in 2–5 cm, moderate roundness, sub-round–subangular 2 m

3. 12.6–15.6 m Brownish yellow, yellowish brown moderate-thick mudstone, interbeded with grayish white thin calcareous mudstone. For the latter, rock consolidation degree is high, hardness is large and bedding is developed 3 m

4. 15.6–46m Brownish yellow, yellowish brown thick bedded mudstone, clear bedding can be seen, individual layer thickness is greater than 2m, the rock is not well cemented, easy weathering, gravel layer is interbeded, abundant mammal fossils can be seen at the bottom 28.4 m

3.2 Mammal fossils

Fossils are located in fourth layer of brown, yellowish brown thick-bedded mudstone, with gravel layer in the upper part. Animal skull, jaw, small joints, bone plate and bone fragment fossils can be seen in mudstone. Two well preserved animal skulls are wrapped by mudstone. One lower jaw bone with completed teeth can be seen, with mudstone in the lower part and gravel in the upper part. Thick animal bone is flattened and crushed. Crystalline

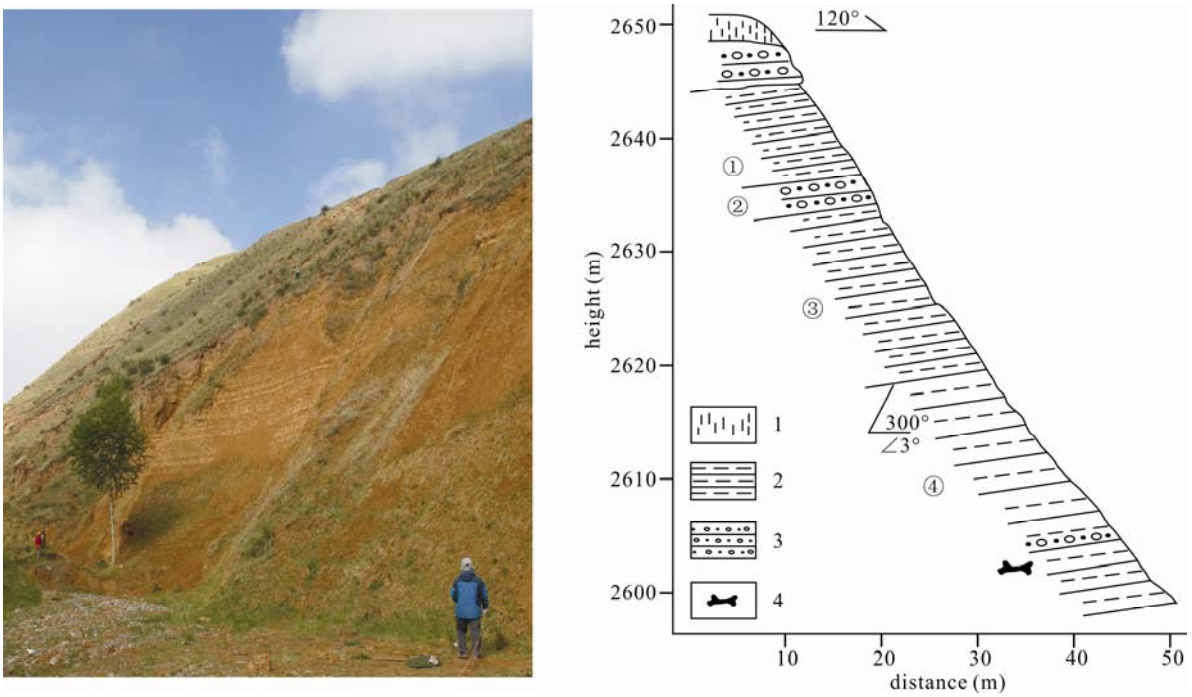

Fig. 2. Banyan profile and the location of the fossil.
1, loess; 2, mudstone; 3, sandy gravel; 4, fossil.

calcite can be seen in well preserved bone. Small joint fossil is well preserved, with obvious joint structure. Fossils are distributed in a range of tens of square meters. Milky bone fossil fragments can be seen in mudstone. The skull fossil and teeth fossils were repaired in the Institute of Vertebrate Paleontology and Paleoanthropology, Chinese Academy of Sciences. The skull is well preserved and the teeth are completed, with obvious enamel gloss in crown. Based on teeth, the skull cheek teeth fossil was identified as *Chilotherium* sp. (Fig. 3a). The teeth fossils were *Hipparion dongxiangense* (Fig. 3b), *Stephanocemas* sp. (Fig. 3c) and *Kubanochoerus* sp. (Fig. 3d) (The fossils were identified by associate professor Wang Yuan and Pro. Jin Changzhu in the Institute of Vertebrate Paleontology and Paleoanthropology, Chinese Academy of Sciences, 2017).

3.3 Sampling and measurement

The thickness of Banyan profile is 46 m. In order to assure the accuracy of paleomagnetic measurement results, high density sampling with an interval of 0.2 m was carried out. When samples were collected in the field, the surface layer of the profile was removed (about 10 cm) in order to get fresh surface. One profile thickness was marked at each 5 sampling points. The horizontal plane was then made at sampling position. The north direction was marked in horizontal plane with calibrated compass by natural azimuth orientation method. The tightly cemented samples were collected by iron shovel. One sample was controlled in a size of 10×10×10 cm in order to be processed to 1 or 2 parallel samples. For fragile samples, two 2×2×2 cm cubes were made on the profile and then the cubes were fastened with a non-magnetic plastic box. Finally, the samples were taken off and marked with direction and sample number. The laboratory processing of the samples was completed by manual cutting. The samples were cut into the cubes with a size of 2.2 cm, then the cubes was carefully grinded to the standard cube samples with a size of 2×2×2 cm by 60-mesh sand paper. Each sample was processed to 1 or 2 parallel samples for test. A total of 176 paleomagnetic samples were collected, with 59 massive samples and 117 non-magnetic plastic box-packed samples.

3.4 Magnetic mineralogy

In order to find out the main occurrence minerals of characteristic remanence, rock magnetism experiment of saturated isothermal remanence curve (IRM) was performed aimed at two selected representative samples. The whole test process was completed in the Labortary of Paleomagnetism, Institute of Geomechanics, Chinese Academy of Geological Sciences. The specific process is as follows : firstly, 10, 20, 40, 60, 100, 150, 200, 300, 400, 500, 600, 700, 800, 900, 1000, 1400, 1800, 2200, 2500 mT field strength was forced on samples with IM-10-30 pulse magnetometer. After field strength was forced, the IRM was measured in AGICO JR-6 rotary magnetometer. Then, -10, -20, -40, 60, -100, -150 mT field strength was

Fig. 3. Teeth fossils discovered in Banyan profile in the Xining basin.
(a), *Hipparion dongxiangense*; (b), *Hipparion dongxiangense*; (c), *Chilotherium* sp.; (d), *Kubanochoerus* sp.; (e), *Parelasmotherium* sp.; (f), *Stephanocemas* sp..

forced on samples in a reverse order. Finally, remanence was measured in order to obtain the saturated isothermal remanence curve of part samples and the demagnetization curve of reverse field (Fig. 4).

In general, the remanence strength of most ferrous magnets was saturated in a magnetic field of 100 mT. The low-coercivity ferromagnetic mineral magnetite and maghem itereached a saturation state in a magnetic field of about 300 mT and remanence coercivity ranged between $(0.56–2.39)\times10^3$ A/m and $(23.89–31.85)\times10^3$ A/m. The saturated magnetic field of hematite and goethite with high coercivity was above 1.5–5.0 T and 5.0 T, and remanence coercivity was 605×10^3 A/m. As shown in the isothermal remanence curve in Fig. 4, the IRM of all the test samples

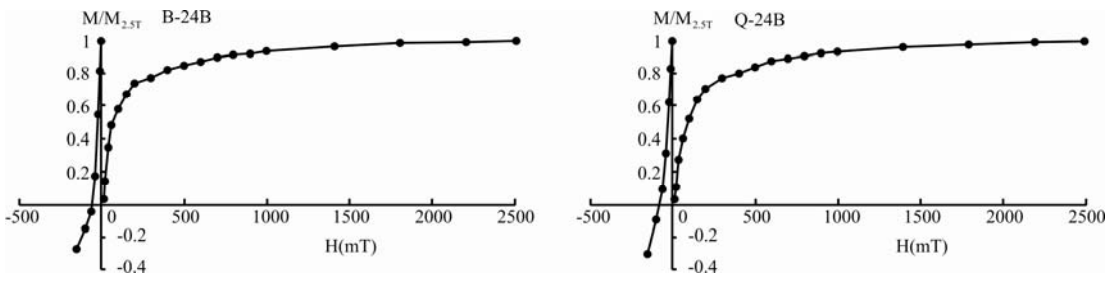

Fig. 4. Normalized IRM acquisition and backfield curves of representative samples.
H, intensity of DC field; M, intensity of remnant magnetization; M2.5T, DC field is 2.5T.

rapidly rose to 70%–78% at 300 mT and was closed to saturated state at 500 mT. Moreover, the magnetization intensity dropped to 0 in a reverse magnetic field of -40–-60mT, indicating remanent bearing minerals were dominated by the magnetite with low coercivity, with minor hematite and goethite with high coercivity.

3.5 Paleomagnetism

The secondary remanence of plastic box-packed samples was cleaned out with alternating demagnetization method and a total of 185 samples were involved in alternating demagnetization (duplicate sample comparative test). The demagnetizing instrument used this time was Molspin alternating demagnetizer with the maximum alternating field strength of 1000 Oe (0.1 T). Since the coercivity of magnetic minerals represented normal logarithmic distribution, demagnetization was gradually completed by the step of the intensity peak of alternating demagnetization magnetic field NRM, 5, 10, 15, 20, 25, 30, 35, 40, 50, 60, 80 and 100 mT. Remanence measurement was performed on 2G-755R typed superconductive magnetometer, with a measurement range of 1.0×10^{-12}–2.0×10^{-4} Am^2 and a sensitivity of 1.0×10^{-12} Am^2. All samples were tested at the Laboratory of Paleomagnetism, School of Earth Sciences and Engineering, Nanjing University. Fig. 5 is the orthogonal vector projection diagram of representative alternating demagnetization samples, it can be seen that alternating demagnetization can only decay the remanence to 25% of NRM. The remanence of most samples was constituted by two magnetic components: at a range of NRM–10 mT, remanence strength decayed to about 70% and vector direction was changed; at 10–40mT, remanence strength decayed to about 70% – 40% and vector direction tended to origin point. It was inferred that the vector of the second part basically represented the characteristic remanence of the samples.

For 2×2×2 cm cube samples, thermal demagnetization means were adopted to clean secondary remanence. A total of 66 samples were involved in alternating demagnetization (duplicate sample comparative test). In order to facilitate the preparation of the overall demagnetization scheme, 15 representative samples were selected in each formation as the pilot samples for intensive demagnetization process in order to understand the demagnetization characteristics of different samples. Thermal demagnetization was completed with the TD-48 thermal demagnetization oven that was produced by US ASC Scientific Inc. According to the test results of the pilot samples, most samples occurred stable demagnetization at a temperature of 350–575°C, a small number of samples occurred completed demagnetization at a temperature of 680°C, and the other samples occurred systematic demagnetization at a temperature order of NRM, 100, 150, 200, 250, 300, 350, 400, 450, 500, 525, 550, 575, 600, 625, 650 and 680°C. Then, remanence measurement was performed with 2G-755R superconductive magnetometer. Generally, when the sample's remanence strength didn't reach 5% of natural remanent magnetization (NRM), it was determined that the remanence was substantially eliminated. All the samples were tested in the Laboratory of Paleomagnetism, School of Earth Sciences and Engineering, Nanjing University. Systematic thermal demagnetization showed

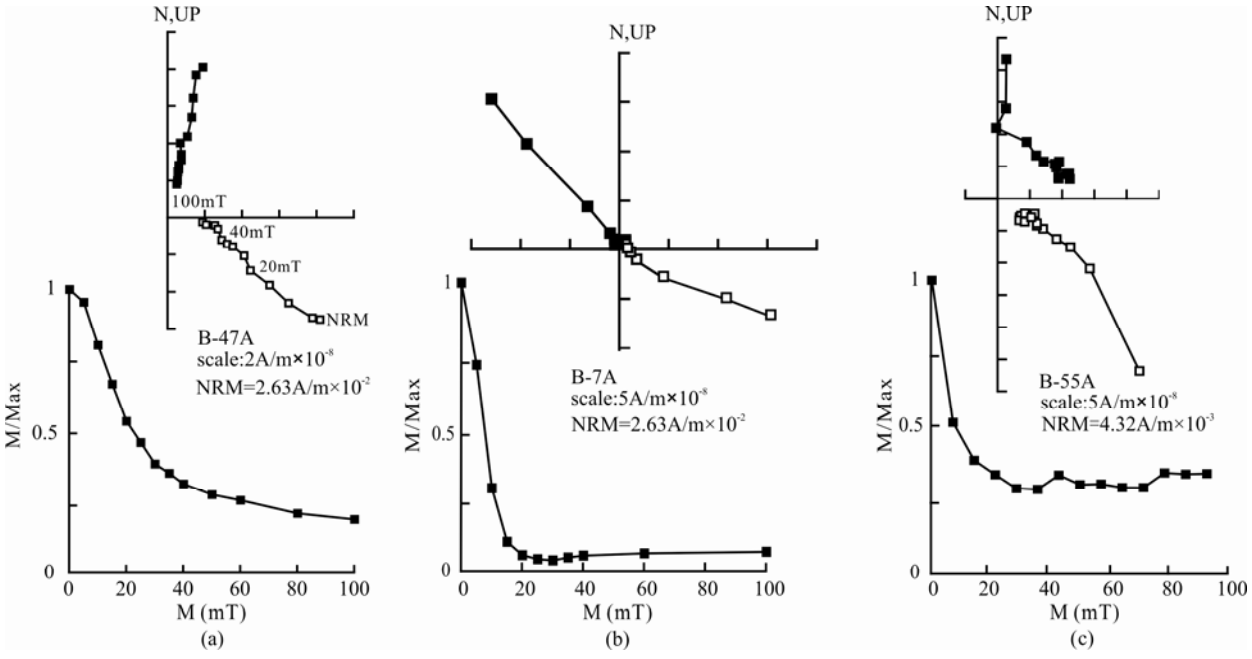

Fig. 5. Alternating demagnetization orthogonal vector projection of the representative samples of Banyan profile.

that the natural remanence strength of the samples in Banyan profile ranged between 10^{-3}–10^{-2} A/m, and the overall thermal demagnetization effect was good. Most samples obtained obvious characteristic remanence, which were divided into two types. One type was single component sample (Fig. 6c), for which, the remanence curve did not change significantly from low temperature to high temperature, showing a single remanence direction (Fig. 6). The other type was double component sample. The low temperature component should be the viscous remanence formed by modern geomagnetic field, which was at a temperature of below 300°C (Fig. 6a). High temperature component had significantly changed remanence strength and direction, which was at a temperature of above 400°C (Fig. 6b). High-temperature demagnetization vector direction stably tended to the origin and remanent strength decreased to the minimum value, representing the direction of characteristic remanence.

3.6 Paleomagnetic measurement results

After the remanence curve was obtained in each temperature interval in all samples, principal component analysis method was used to calculate the declination and inclination of samples (Kirschvink, 1980) (Fig. 7). In order to assure the reliability and accuracy of the data, the data with low reliability were eliminated according to the following principles: (1) The samples with disordered and unstable demagnetization curves and without effective characteristic remanence; (2) The samples with the confidence circle half apex α95 of characteristic remanence of greater than 5, even greater than 10. A total of 251 samples were tested, among which, 45 samples were eliminated, accounting for 18% of the total samples. The eliminated points were dispersedly distributed in each interval, so the accuracy of the magnetic pole of the profile was not affected.

After the declination and inclination of the samples of Banyan profile were obtained by characteristic remanence, the latitude of the virtual magnetic pole (VGP) was calculated by Pmcalc software. Then, the VGP of all the samples was plotted in order to obtain the geomagnetic polarity reversal sequence of the profile. Finally, the geomagnetic polarity reversal sequence of the profile was compared to standard magnetic polarity chronology (Hilgen et al, 2012) (Fig. 7). The study results of magnetic stratigraphy showed that there were five positive polar segments (N1–N5) and five negative polar segments (R1–R5) in Banyan profile. Since the age of mammal fossils was late Miocene, when the obtained paleomagnetic polarity column was compared to the late Miocene segment of slandered polarity column, the variation of long polarity N4 corresponded to the C4n.2n of standard polarity column, the interval characteristics of other positive polar segments (N1–N5) were consistent with C3Br.1n–C4r.1n event and their positive polarity corresponded to C3Br.1n, C3Br.2n, C4n.1n, C4n.2n, C4r.1n of standard magnetic polarity column.

The age of top Banyan profile N1 was about 7.25 Ma calculated by a depositional rate of C3Br. The age of

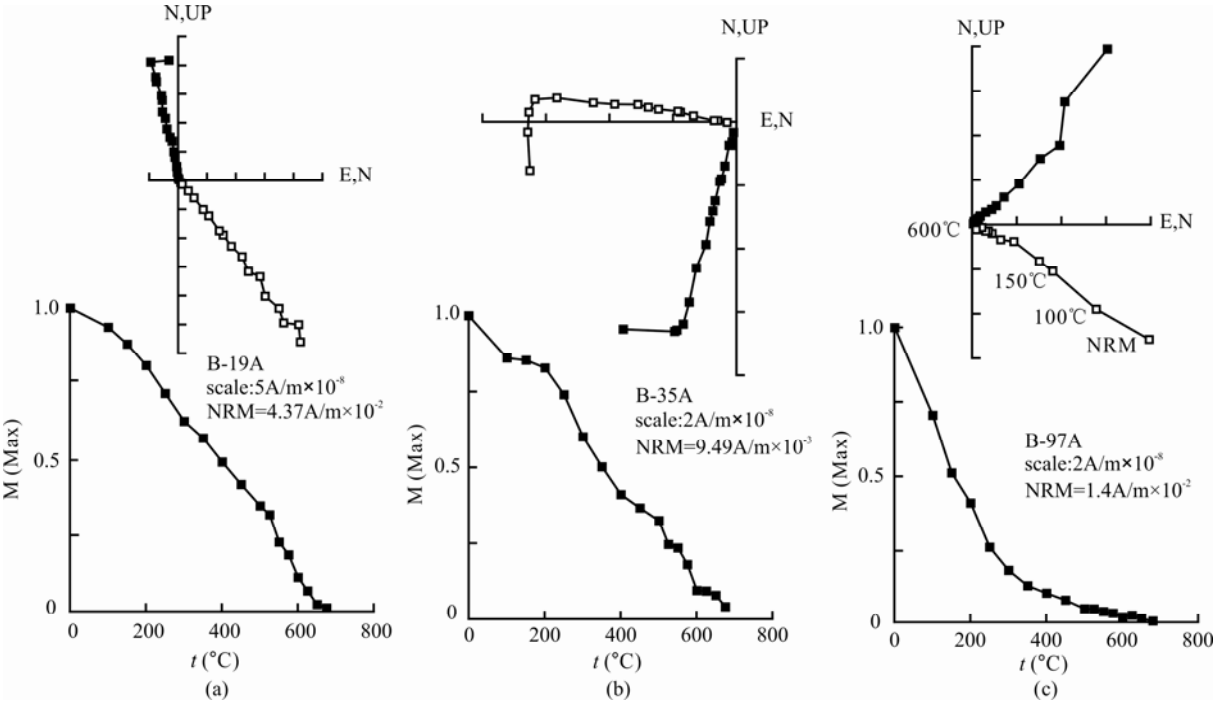

Fig. 6. Thermal demagnetization orthogonal vector projection of the representative samples of Banyan profile.

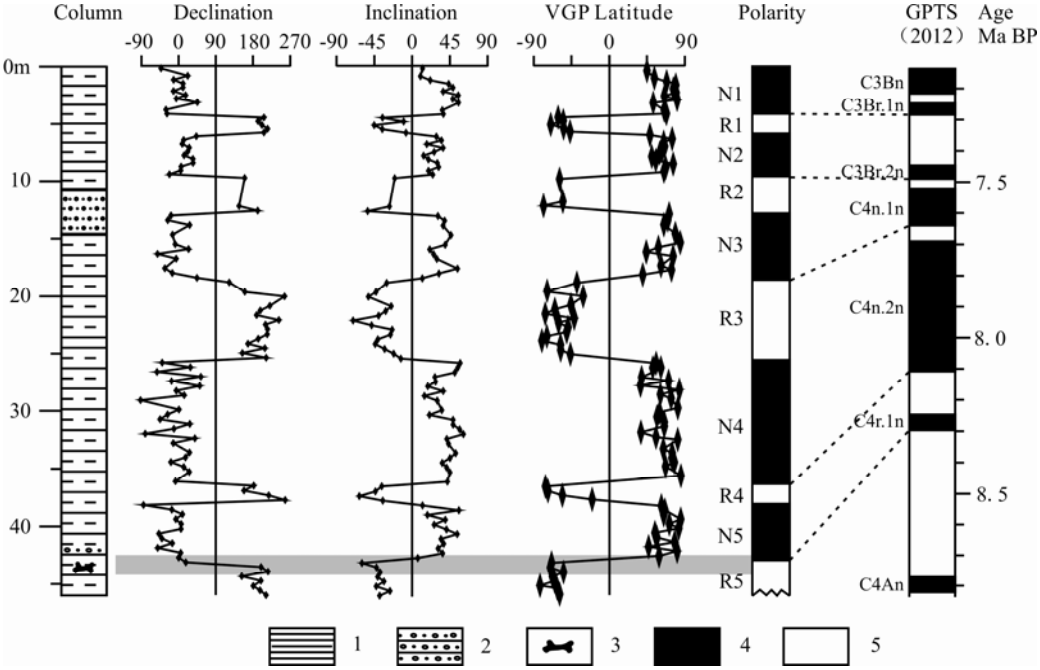

Fig. 7. Paleomagnetic measurement results of Banyan profile.
1, mudstone; 2, sandy gravel; 3, fossil; 4, normal polarity; 5, reversed polarity.

bottom Banyan profile was about 8.4 Ma which calculated by at a depositional rate of C4n.1n. The age range of Banyan profile was 1.15 Ma. The discovered fossils were exposed between N5 and R5 at the bottom of Banyan profile, so the age of mammal fossil layer was calculated to be about 8.3 Ma.

4 Discussion

4.1 Characteristics of mammal fossil

According to the identification results of Jin Changzhu and Wang Yuan from the Institute of Vertebrate Paleontology and Paleoanthropology, Chinese Academy of Sciences, the age of the paleontological fossils, including *Hipparion dongxiangense*, *Chilotherium* sp., *Parelasmotherium* sp., *Stephanocemas* sp. *and Kubanochoerus* sp. discovered in Jiangjiagou and Shagou of Banyan Valliage in Huzhu area, Xining basin was early Late Miocene.

The age of the Xiejia fauna, Danshuilu district fauna and Diaogou district mammal fauna discovered in the Xining Basin was early Miocene, early Middle Miocene and late Middle Miocene, respectively (Fig. 8). Among the fossil community existed in the Xining basin, Diaogou mammal fauna had the closest age to the discovered fossils. The main paleontology was *Gomphotherium wimani, G.connexus*, *Elasmofherini*, *Rhinocerotidae indet*, *Stephanocemas chinghaiensis*, *Alloptox chinghaiensis*, *Plesiodipus leei*, *Micromerys* sp., *Bunolistriodon minheensis*. (Li Chuankui et al, 1980; Li Chuankui et al., 1981). The fossils discovered in Banyan included *Hipparion dongxiangense*, *Chilotherium* sp., *Parelasmotherium* sp., *Stephanocemas* sp. *and Kubanochoerus* sp.. The fossil species were significantly different from Diaogou fauna. The age of Banyan paleontology, including *Hipparion dongxiangense,* and *Chilotherium* sp. was significantly later than that of Diaogou mammal fauna, which was consistent with the test results of paleomagnetic chronology. At the same time, the discovery of paleontological fossils also filled the blank that the Xining basin was lack of late Miocene mammal fauna.

4.2 Regional comparison of mammal fossils

Regionally, the Xining basin was a sub-basin of Longzhong sedimentary basin in Paleogene-Neogene and it also covered adjacent basins, such as Linxia basin, Lanzhou basin and Jianzha. Affected by the remote effect of the compression of Qinghai-Tibet Plateau at early stage, there was similar tectonic and sedimentary environment between the basins. Therefore, the late Miocene mammal fossils discovered in the Xining basin should also appear in adjacent basins.

Previous studies (Zhang Xing, 1993) showed that there were mammal fossils in the late Miocene strata of fluvial-lacustrine facies in Longgushan, Xingjiawan, Yongdeng County, Lanzhou basin, including *Hipparion* sp., *Chilotherium haberei*, *Cervidae indet.*, *Chleuastochoerus*

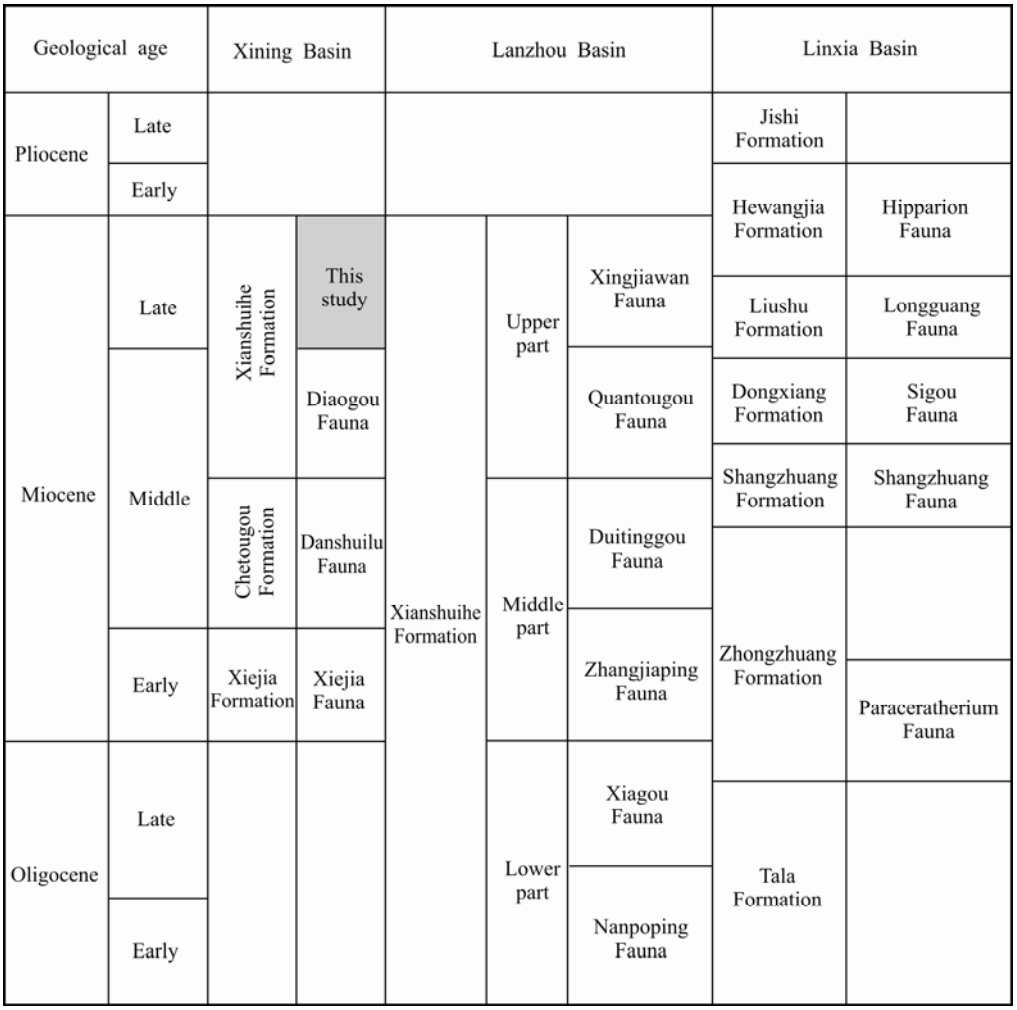

Fig. 8. The stratigraphic correlation of the Longzhong basin (modified from Zhang Peng et al., 2016). The age of Xining basin is based on Dai et al. (2006) and Li Chuankui et al. (1981), Lanzhou basin on Qiu Zhanxiang et al. (1997) and Xie Guangpu (2004), Linxia basin on Fang et al. (2003).

stehlini, *Stegodon* sp., *Hyeana variabilis*. Their latest paleomagnetic age was about 8 Ma (Ao et al., 2016). The paleontological fossils discovered in Xingjiawan were well consistent with the *Hipparion* sp., *Chilotherium haberei* and *Cervidae indet*. Discovered in Xining, thereby the fauna of the two places should be the product of the same age.

The mammal fossils of the Linxia basin had been deeply studied. The age of *Platybelodon* fauna and *Hipparion* fauna was during in Miocene. The *Hipparion* fauna of middle Late Miocene was discovered in Liushu Formation, including *Gliroid rodents, carnivores, Hipparion sp., H.dongxiangense, H.chiai*, *H.weihoense*, *H.coelophyes*, *H.dermatorhinum*, *Tetralophodon* sp., *T.exoletus*, *Acerorhinus hezhengensis, Chilotherium wimani, Iranotherium morgani, Parelasmotherium simply, P.linxiaense, Dicerorhinus ringstromi, Chleuastochoerus stehlini, Microstonyx major, Dicrocerus* sp., *Cervavitus novorossiae* (Deng Tao et al., 2004). The paleomagnetic age was 13.07–7.78 Ma (Fang Xiaomin et al., 2007). The fossils discovered in Banyan profile was *Hipparion dongxiangense, Chilotherium* sp., *Parelasmotherium* sp., *Stephanocemas* sp. and *Kubanochoerus* sp.. The fossil species were similar with the *Hipparion* fauna of the Linxia basin, but less in number, reflecting there were some differences in basin environments in the same period. With the basin extending to the plateau, the living environment gradually became worse.

4.3 Stratigraphic significance

The Cenozoic sedimentary strata in the Xining basin were not able to be dated using traditional isotope method due to the lack of the volcanic strata required by isotopic dating. Therefore, the paleomagnetic and paleontological methods became the main means to determine the stratigraphic sedimentary age of the basin. Existed basin magnetic chronology study was mainly focused on the Xiejia profile, Tashan profile and Shuiwan profile in

southern-central basin. Due to the erosion at the top of the profile, Wu Lichao (2006) measured the age of Xiejia profile as 15.01–24.22 Ma based on paleomagnetic method and the upper age of Xianshuihe Formation at profile top was 15.01 Ma. Dai et al., (2006) carried magnetic stratigraphic study in the Xiejia profile and Shuiwan profile in the southern and central Xining basin and measured the paleomagnetic age of Qijiachuan Formation, Honggou Formation, Mahalagou Formation, Xiejia Formation, Chetougou Formation and Xianshuihe Formation in the Xining basin as 52.5–0 Ma, 50–41.5 Ma, 41.5–30 Ma, 30–23 Ma, 23–18 Ma and 18 Ma–<17 Ma (Dai, et al., 2006) respectively.

In 2012, Fang Xiaomin's team took the cores with a length of 194 m in Tashan. The paleomagnetic measurement results showed that the age of Tashan borehole was 18.5–13.5 Ma, so the upper age of the stratigraphic age of Xianshuihe Formation was further expanded (Zan, et al., 2015). The paleomagnetic age of Banyan profile was 7.25–8.4 Ma, indicating the strata represented by Banyan profile were the Xianshuihe Formation of late Miocene. The upper age of the stratigraphic age of Xianshuihe Formation would be further expand if the Xianshuihe Formation in Jiangjiagou and Banyan area was deeply investigated, thereby more completed sedimentary stratigraphic and palaeontological data would be provided for studying the late Cenozoic strata of the Xining basin and regional environmental correlation.

4.4 Tectonic significance

The Cenozoic tectonic uplifting of the Qinghai-Tibet Plateau was an important process in the tectonic evolution of China. Many scholars had tried to restrict the uplifting process of the Qinghai-Tibet Plateau using the methods of low temperature thermochronology, paleontology-palaeoclimate, sedimentary palaeogeography and sedimentary stable isotopes. It was important to restrict the uplifting of the plateau using paleontological fossils. Xu Ren et al. discussed the uplifting time of the plateau using *Quercus semicarpifolia* fossil (Xu Ren et al., 1973). Previous studies showed that Laji Mountain that divided the Xining basin and the Guide basin was not formed in Eocene, so the Xining basin and the Guide basin was not independence lake basin (Fang Xiaomin et al., 2007; Wang Guocan et al., 2011). Laji Mountain and Zhaimazari Mountain began to uplift in Miocene (23–21 Ma). The Xining basin, Guide basin and Xunhua basin began to break up, forming separated lake basin. Since 8 Ma, Laji Mountain began to intensively uplift, so the lacustrine deposits of northern Guide basin rapidly transited into alluvial-pluvial pan deposits. The present tectonic geomorphic pattern of interior plateau was formed after another rapid uplifting occurred in 3.6 Ma. The late Miocene mammal fossils were discovered in interior Xining basin. Regional paleontological comparison results showed that the Xining basin had similar paleontological and paleoclimatic conditions with surrounding Lanzhou basin and Linxia basin. The elevations of fossil sites are difference among Hualin, Hezheng County, Linxia basin, and Xingjiawan, Yongdeng County, Lanzhou basin and this site. The most height difference more than 500m (Table 1), and the uplift height of Xining basin area is greater than Lanzhou basin area. It shows that uplift of Tibetan Plateau is different in difference regions after late Miocene. It is believed that the Qinghai-Tibet Plateau rapidly uplifted in the late Late Cenozoic (Xu Ren et al., 1973; Li Jijun et al., 1979; Molnar et al., 1993; Li Tingdong, 1995; Meyer et al., 1998; Tapponnier et al., 2001; Wang et al., 2003; Zhu Dagang et al., 2006; Zhang Peizhen et al., 2006). The discovery of mammal fossils and the results of palaeomagnetic chronology in this paper also support this view. Therefore, the discovery of the paleontological fossil supported the fact that Xining and Guide interior plateau basin were rapidly uplifted after 8.3 Ma.

5 Conclusion

(1) The mammal fossils, including *Hipparion dongxiangense, Chilotherium* sp., *Parelasmotherium* sp., *Stephanocemas* sp. *and Kubanochoerus* sp. were discovered in Jiangjiagou and Banyan in Huzhu County, Xining basin and their age was identified as early Late Miocene. The discovery of the fossils filled the blank that there were no large mammal fossils in the Xining Bain in Late Miocene.

(2) The study results of magnetic stratigrapy showed that five positive polarity segments (N1–N5) and five negative polarity segments (R1–R5) were recorded in Banyan profile. The five positive polarity segments corresponded to C3Br.1n, C3Br.2n, C4n.1n, C4n.2n and C4r.1n in standard polarity segment. The paleomagnetic age range of Banyan profile was 1.15 Ma (7.25–8.4 Ma).

Table 1 Elevation contrast of mammal fossils site point between Xining and its adjacent basins

Basin	Site	Longitude	Latitude	Altitude
Xining basin	Banyan, Huzhu county	E102°6.000′	N36°41.00′	2645 m
Linxia basin	Hualin, Hezhen county	E103°24.97′	N35°41.76′	2318 m
Lanzhou basin	Xingjiawan, Yongdeng county	E103°0.100′	N36°41.42′	2149 m

Mammal fossils were discovered between positive polarity N5 and Negative polarity R5 and their paleomagnetic age was 8.3 Ma.

(3) The late Miocene mammal fossil assemblage of the Xining basin represented by *Hipparion dongxiangense, Chilotherium* sp.*, Parelasmotherium* sp.*, Stephanocemas* sp. and *Kubanochoerus* sp. was consistent with the paleontological fossils of Xingjiawan in the Linxia and Lanzhou basin, indicating each basin had similar climate and environmental condition in late Miocene.

(4) The discovery of the paleontological fossils proved that the northeastern margin of the Qinghai-Tibet Plateau rapidly uplifted in late Miocene after 8.3 Ma, which was consistent with the understandings that the Qinghai-Tibet Plateau occurred rapid uplifting at the late stage of late Cenozoic.

Acknowledgements

This work granted by the National Natural Science Foundation of China (Grant No. 41772381), the Chinese Academy of Geological Sciences Research Fund (Grant Nos. YYWF201511 and DZLXJK201710) and the Geological Investigation Project of China Geological Survey (Grant Nos. 121201234000160014, 12120113006100, 121201104000150009 and DD20160083). Thanks Pro. Jin Changzhu and associate professor Wang Yuan and Sun Wenshu, Institute of Vertebrate Paleontology and Paleoanthropology, Chinese Academy of Sciences, for repairing and identifying the mammal fossils. Thanks local villager Lü Youjin for collecting fossils in field. Thanks Pro. Wang Xisheng, Institute of Geomechanics, Chinese Academy of Geological Sciences, for his help with paleomagnetism.

Manuscript received Dec. 21, 2017
accepted Mar. 27, 2018
edited by Liu Lian

References

Abels, H.A., Dupont-Nivet, G., Xiao, G.Q., Bosboom, R., and Krijgsman, W., 2011. Step-wise change of Asian interior climate preceding the Eocene–Oligocene transition (EOT). *Palaeogeography Palaeoclimatology Palaeoecology*, 299(3–4): 399–412.

Ao, H., Zhang, P., Dekkers, M.J., Roberts, A.P., An, Z.S., Li, Y.X., Lu, F.Y., Lin, S., and Li, X.W., 2015. New magnetochronology of Late Miocene mammal fauna, NE Tibetan Plateau, China: Mammal migration and paleoenvironments. *Earth and Planetary Science Letters*, 434: 220–230.

Bosboom, R.E., Abels, H.A., Hoorn, C., Berg, B.C.J., Guo, Z.J., and Dupont-Nivet, G., 2014. Aridification in continental Asia after the middle Eocene climatic optimum (MECO). *Earth and Planetary Science Letters*, 389: 34–42.

Bureau of Geology and Mineral Resources of Qinghai Province, 1991. *Regional Geology of Qinghai Province*. Beijing: Geological Publishing House, 1–604 (in Chinese).

Chen Chuanfei, Miao Yunfa, Fang Xiaomin, Song Chunhui, Dai Shuang, Yan Xiaoli, Zhang Qibo, Xu Li and Xia Weimin, 2009. The Discovery and Significance of the Fossil Woods in the Bottom of Chetougou Formation in Xiejia Section, Xining Basin. *Acta Geologica Sinica*, 83(8): 1104–1109 (in Chinese with English abstract).

Dai, S., Fang, X., Dupont-Nivet, G., Song, C., Gao, J., Krijgsman, W., Langereis, C., and Zhang, W., 2006. Magnetostratigraphy of Cenozoic sediments from the Xining Basin: Tectonic implications for the northeastern Tibetan Plateau. *Journal of Geophysical Research*, 111, B11102, doi: 10. 1029/ 2005JB004187.

Deng Tao, Wang Xiaoming, Ni Xijun, Liu Liping and Liang Zhong, 2004. Cenozoic stratigraphic sequence of the Linxia Basin in Gansu, China and its evidence from mammal fossils. *Vertebrata Palasiatica*, 42(1): 45–66 (in Chinese with English abstract).

Dupont-Nivet, G., Krijgsman, W., Langereis, C.G., Abels, H.A., Dai S., and Fang X.M., 2007. Tibetan plateau aridification linked to global cooling at the Eocene-Oligocene transition. *Nature*, 445(7128): 635–638.

Fang, X.M., Garzione, C., Van der Voo, R., Li, J.J., and Fan, M.J., 2003. Flexural subsidence by 29 Ma on the NE edge of Tibet from the magnetostratigraphy of Linxia Basin, China. *Earth and Planetary Science Letters*, 210(3): 545–560.

Fang Xiaomin, Song Chunhui, Dai Shuang, Zhu Yingtang, GaoJunping and Zhang Weilin, 2007. Cenozoic deformation and uplift of the NE Qinghai-Tibet Plateau: evidence from high resolution magnetostratigraphy and basin evolution. *Earth Science Frontiers*, 14(1): 230–242(in Chinese with English abstract).

Han Jian'en, Chen Qiguang, Meng Xiangang, Zhu Dagang, Zhang Qianqian, Quan Kai, Wang Jin and Xu Biao, 2015. Discovery and significance of Hipparion and parelasmotherium fossiles in the Xining Basin, Qinghai Province. *Acta Geoscientica Sinica*, 36(1): 115–120 (in Chinese with English abstract).

Han Jian'en, Shao Zhaogang, Xu Biao, Zhang Qianqian, Yu Jia, Meng Qingwei, Meng Xiangang, Zhu Dagang and Wang Jin, 2017. First report of late Miocene mammals including Chilotherium in the Xining Basin, NE Tibetan Plateau, China. *Acta Geologica Sinica* (English Edition), 91(3): 1135–1136.

Hilgen, F., Lourens, L., and Van Dam, J., 2012. The Neogene period. In: Gradstein, F.M., Ogg, J.G., Schmitz, M.D., Ogg, G.M. (eds.), *The Geologic Time Scale*. Am-sterdam: Elsevier, 923–978.

Horton, B.K., Dupont-Nivet, G., Zhou, J.,Waanders, G.L., Butler, R.F., and Wang, J., 2004. Mesozoic-Cenozoic evolution of the Xining-Minhe and Dangchang basins, northeastern Tibetan Plateau: Magnetostratigraphic and biostratigraphic results. *Journal of Geophysical Research*, (109): 657–681.

Kirschvink, J.L., 1980. The least-squares line and plane and the analysis of palaeomagnetic data. *Geophysical Journal International*, 62(3): 699–718.

Li Chuankui and Qiu Zhuding, 1980. Early Miocene mammalian fossils of Xining Basin, Qinghai. *Vertebrata Palasiatica*, 18 (3): 198–215 (in Chinese with English abstract).

Li Chuankui, Qiu Zhuding and Wang Shijie, 1981. Discussion on Miocene stratigraphy and mammals from Xining Basin, Qinghai. *Vertebrata Palasiatica*, 19(4): 313–320 (in Chinese with English abstract).

Li Tingdong, 1995. The uplifting process and mechanism of the Qinghai-Tibet plateau. *Acta Geoscience Sinica*, 16(1): 1–9 (in Chinese with English abstract).

Li Jijun, Wen Shixuan, Zhang Qingsong, Wang Fubao, Zheng Benxing and Li Bingyuan, 1979. On the timing, scope and styles of the uplift of the Tibetan Plateau. *Science in China*, 9 (6): 608–616 (in Chinese with English abstract).

Liu Mengru, 1992. Stratigraphic sequence and fossil assemblage of Neogene system in Xining-Minhe basin. *Qinghai Geology*, (2): 1–18 (in Chinese with English abstract).

Meyer, B., Tapponnier, P., Bourjot, L., Métivier, F., Gaudemer, Y., Peltzer, G., Guo, S.M., and Chen, Z.T., 1998. Crustal thickening in Gansu-Qinghai, lithospheric mantle subduction, and oblique, strike-slip controlled growth of the Tibet Plateau. *Geophysical Journal International*, 135(1): 1–47.

Molnar P., England P., and Martinod J., 1993. Mantle dynamics, uplift of the Tibetan plateau, and the Indian monsoon. *Reviews of Geophysics*, 31: 357–396.

Qiu Zhanxiang, Wang Banyue and Qiu Zhuding, 1997. Recent advances in study of the Xianshuihe Formation in Lanzhou Basin. In: Tong Yongsheng, *Evidence for evolution: Essays in honor of Prof. Chungchien Young on the hundredth anniversary of his birth*. Beijing: China Ocean Press: 177–192 (in Chinese).

Sun Xiuyu, Zhao Yingniang and He Zhuosheng, 1984. The Oligocene-Miocene palynological assemblages from the Xining-Minhe basin, Qinghai Province. *Geological Review*, 30(3): 2074–216 (in Chinese with English abstract).

Tapponnier, P., Zhiqin, X., Roger, F., Meyer, B., Arnaud, N., Wittlinger, G., and Yang, J.S., 2001. Oblique stepwise rise and growth of the Tibet Plateau. *Science*, 294(5547): 1671–1677.

Wang Guocan, Cao Kai, Zhang Kexin, Wang An, Liu Chao, Meng Yanning and Xu Yadong, 2011. Spatio-temporal framework of tectonic uplift stages of the Tibetan Plateau in Cenozoic. *Science China Earth Science*, 41(3): 29–44 (in Chinese with English abstract).

Wang, E., Wan, J., and Liu, J., 2003. Late Cenozoic geological evolution of the foreland basin bordering the West Kunlun range in Pulu area: Constraints on timing of up lift of northern margin of the Tibetan Plateau. *Journal of Geophysical Research*, 108 (B8): 2401–2413.

Wu Lichao, Yue Leping, Wang Jianqi, Heller F., and Deng Tao, 2006. Magnetostratigraphy of stratotype section of the Neogene Xiejian stage. *Journal of Stratigraphy*, 30(1): 50–53 (in Chinese with English abstract).

Xiao, G.Q., Abels, H.A., Yao, Z.Q., Dupont-Nivet, G., and Hilgen, F. J., 2010. Asian aridification linked to the first step of the Eocene-Oligocene climate transition (EOT) in obliquity -dominated terrestrial records (Xining Basin, China). *Climate of the Past*, 21(1): 219–220.

Xiao, G.Q., Guo, Z.T., Dupont-Nive,t G., Lu, H.Y., Wu, N.Q., Ge, J.Y., Hao, Q.Z., Peng, S.Z., Li, F.J., Abels, H. A., and Zhang, K.X., 2012. Evidence for northeastern Tibetan Plateau uplift between 25 and 20 Ma in the sedimentary archive of the Xining Basin, Northwestern China. *Earth and Planetary Science Letters*, 317–318: 185–195.

Xie Guangpu, 2004. The tertiary and local mammalian faunas in Lanzhou Basin, Gansu. *Journal of Stratigraphy*, 8(1): 67–80 (in Chinese with English abstract).

Xu Li, Miao Yufa, Fang Xiaomin, Song Chunhui, Xia Weimin, Yan Xiaoli, Han Wenxia, Zhang Qibo, Chen Chuanfei and Dai Shuang, 2009. Middle Eocene-Oligocene climatic changes recorded by sedimentary colors in the Xining Basin, in Northeastern Tibetan Plateau, NW China. *Journal of Lanzhou University* (Natural Sciences), 45(1): 12–19 (in Chinese with English abstract).

Xu Ren, Tao Junrong and Sun Xiangjun, 1973. On the discovery of a Quercus semicarpifolia bed in mountain shishapangma and its significance in botany and geology. *Acta Botanica Sinica*, 15:102–119 (in Chinese with English abstract).

Ye Liusheng, 1976a. The time of Xining formation in Xining-Minhe Basin, Qinghai Province. *Qinghai Geology*, (3): 51–62 (in Chinese).

Ye Liusheng, 1976b. New understanding of the Xining formation. *Northwestern Geology*, 9(3): 68–69 (in Chinese).

Zan, J.B., Fang, X.M., Yan, M.D., Zhang, W.L., and Lu, Y., 2015. Lithologic and rock magnetic evidence for the mid-Miocene climatic optimum recorded in the sedimentary archive of the Xining basin, Tibetan plateau. *Palaeogeography Palaeoclimatology Palaeoecology*, 431: 6–14.

Zhang Peng, Ao Hong and An Zhisheng, 2016. Review of the stratigraphy and paleoclimatology study of the Paleogene–Neogene Longzhong Basin. *Journal of Earth Environment*, 7 (2): 97–120 (in Chinese with English abstract).

Zhang Xing, 1993. New discovery of the mammalian fossils in Baode period of later Miocene Epoch in Lanzhou Basin. *Acta Geologica Gansu*, 2(1): 1–5 (in Chinese with English abstract).

Zhang Peizhen, Zheng Dewen, Yin Gongming, Yuan Daoyang, Zhang Guangliang, Li Chuanyou and Wang Zhicai, 2006. Discussion on late Cenozoic growth and rise of northeastern margin of the Tibetan Plateau. *Quaternary Sciences*, 26(1): 5–13 (in Chinese with English abstract).

Zhu Dagang, Meng Xiangang, Shao Zhaogang, Yang Chaobin, Han Jian'en, Yu Jia, Meng Qingwei and Lü Rongping, 2006. The formation and evolution of Zhada basin in Tibet and the uplift of the Himalayas. *Acta Geoscience Sinica*, 27(3): 193–200 (in Chinese with English abstract).

About the first author

HAN Jian'en, male; born in 1980 in Baoji City, Shaanxi Province; doctor; senior engineer of Institute of Geomechanics, Chinese Academy of Geological Sciences. He is now interested in the study on structural geology, regional geology and global climatic change in Qinghai-Tibetan Plateau. Email: hanjianen@163.com; phone: 010–88815011, 13811332236.